Inorg. Chem. **2008**, *47*, 4591−4595

A Comparison of Neptunyl(V) and Neptunyl(VI) Solution Coordination: The Stability of Cation−Cation Interactions

S. Skanthakumar, Mark R. Antonio, and L. Soderholm*

Heavy Elements and Separation Sciences Group, CSE/200, Argonne National Laboratory, Argonne, Illinois 60439

Received December 21, 2007

The solution coordination environments of pentavalent and hexavalent Np are studied by high-energy X-ray scattering. Np^{5+} and Np^{6+} both exist as the neptunyl moiety coordinated with five equatorial waters at Np−O distances of 2.46(2) and 2.37(2) Å, respectively. NpO_2^{2+} also has a second coordination sphere of 6−10 waters at 4.37(3) Å. The NpO_2^{+} scattering is complicated by the presence of scattering at about 4.2 Å that is attributed to Np−Np cation−cation interactions. The analysis of changing intensity of this peak as a function of Np concentration is used to determine a stability constant of $K_{eq} = 0.74(9)$ M^{-1} for the dimeric complex.

Introduction

Like other high-valent actinide ions, Np^{5+} is found primarily as the linear dioxo ion, NpO_2^{+}.[1] The most prevalent species in aqueous solutions over a wide variety of conditions, the neptunyl(V) ion is generally thought to be noncomplexing, in part because of its small charge-to-radius ratio. In the solid state, it can form layered structures similar to those found for the UO_2^{2+} ion, with the nonbonding dioxo ligands positioned perpendicular to the sheets.[2] However, in contrast to both uranyl(VI) and neptunyl(VI) structural chemistry, the oxo ligands of the neptunyl(V) ion have a propensity to coordinate as an equatorial ligand in the first coordination sphere of a neighboring neptunyl ion, as depicted in Figure 1a. Known as cation−cation interactions (CCIs), such ligation was first reported in solution and involved interactions between NpO_2^{+} and UO_2^{2+} based on the interpretation of optical spectra.[3] Subsequent work reported similar complexes involving the complexation of the monovalent neptunyl(V) ion with a variety of other ions, including Cr^{3+},[4,5] Rh^{3+},[6] $VO^{+/2+}$,[7] Th^{4+},[8] Hg_2^{2+},[9] UO_2^{2+},[10−12] and $NpO_2^{+/2+}$ itself.[8,12,13]

Although CCIs are now well-documented in the solid state, where they are found in a significant fraction of known NpO_2^{+} structures, the verification of this structural motif for ions coupling in solution has been elusive. Optical techniques, including infrared,[11] UV/visible,[13] and Raman[11] spectroscopies, have been used with specific emphasis on determining stability constants. Large-angle X-ray scattering data from a 1.7 M NpO_2^{+} solution in perchloric acid with an ionic strength (IS) of 0.5 M found evidence of a Np−Np interaction with an interatomic distance of 4.2 Å.[12] As noted by the authors, the distance did not yield information sufficient to distinguish the CCI structure depicted in Figure 1a from that of the simple dihydroxy-bridged species shown in Figure 1b. Subsequent studies on a neptunyl nitrate solution using Np L_3-edge extended X-ray absorption fine structure (EXAFS) spectroscopy also found evidence for a Np(V)−Np(V) interaction at about 4.2 Å but were not able to provide any further quantitative information.[14]

Herein, we report the use of high-energy X-ray scattering (HEXS) to study and compare the coordination environments of both NpO_2^{+} and NpO_2^{2+} in a 1 M perchloric acid solution.

* Author to whom correspondence should be addressed. E-mail: LS@anl.gov.

(1) Fahey, J. A. In *The Chemistry of the Actinide Elements*, 2nd ed.; Katz, J. J., Seaborg, G. T., Morss, L. R., Eds.; Chapman and Hall: London, 1986; Vol. *1*, pp 443−498.
(2) Burns, P. C. *Can. Mineral.* **2005**, *43*, 1839–1894.
(3) Sullivan, J. C.; Zielen, A. J. *J. Am. Chem. Soc.* **1961**, *83*, 3373–3378.
(4) Sullivan, J. C. *J. Am. Chem. Soc.* **1962**, *84*, 4256–4259.
(5) Karraker, D. G.; Stone, J. A. *Inorg. Chem.* **1977**, *16*, 2979–2980.
(6) Murmann, R. K.; Sullivan, J. C. *Inorg. Chem.* **1967**, *6*, 892–900.
(7) Madic, C.; Begun, G. M.; Hobart, D. E.; Hahn, R. L. *Radiochim. Acta* **1983**, *34*, 195–202.
(8) Stoyer, N. J.; Hoffman, D. C.; Silva, R. J. *Radiochim. Acta* **2000**, *88*, 279–282.
(9) McKee, M. L.; Swart, M. *Inorg. Chem.* **2005**, *44*, 6975–6982.
(10) Madic, C.; Guillaume, B.; Morisseau, J. C.; Moulin, J. P. *J. Inorg. Nucl. Chem.* **1979**, *41*, 1027–1031.
(11) Guillaume, B.; Begun, G. M.; Hahn, R. L. *Inorg. Chem.* **1982**, *21*, 1159–1166.
(12) Guillaume, B.; Hahn, R. L.; Narten, A. H. *Inorg. Chem.* **1983**, *22*, 109–111.
(13) Stout, B. E.; Choppin, G. R. *Radiochim. Acta* **1993**, *61*, 65–67.
(14) Den Auwer, C.; Grégoire-Kappenstein, A. C.; Moisy, P. *Radiochim. Acta* **2003**, *91*, 773–776.

10.1021/ic702478w CCC: $40.75
Published on Web 05/03/2008

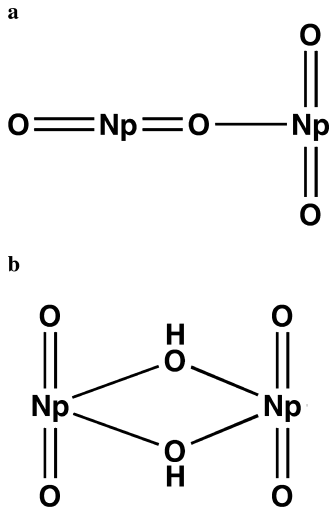

Figure 1. The two models suggested for neptunyl(V) cation−cation interactions: (a) Model I, the T-shaped configuration in which the oxo ligand of one of the Np(V) bonds in the equatorial plane of the adjacent neptunyl ion, and (b) Model II, a dihydroxo-bridged species in which the dioxo moieties are parallel to each other and perpendicular to the plane including the O of the hydroxyl groups.

A comparison of the Np−Np interaction distance with recently published single-crystal structural studies provides further insight into the solution structure of the complex. By electrochemically generating oxidation-state pure neptunyl(VI) species in solution, we are able to directly compare its scattering with that from neptunyl(V) from the same solution. These data are used to extract a stability constant for the CCI complex under the conditions of our experiments that agrees well with those previously obtained by optical spectroscopic techniques.

Experiments

Sample Preparation. ***Caution!*** *^{237}Np represents a serious health risk due to the emission of α and γ radiation as well as β radiation from its primary decay product. Such studies require appropriate infrastructure and personnel training in the handling of radioactive materials.*

A standard 0.4 M ^{237}Np in 1 M $HClO_4$ solution was used for all experiments with the IS constant at 1 M. Solution concentrations were confirmed via optical, coulometric, and scintillation techniques. A BASi 100B/W electrochemical workstation was used for the controlled-potential electrolysis (with coulometry) of a purified, green neptunyl(V) aqua ion solution.[15] Exhaustive (99.9%) oxidation was achieved after 37 min with the electrode polarized at +1.20 V, an effective potential as employed beforehand,[16] resulting in a deep-pink neptunyl(VI) solution.

X-Ray Scattering. The high-energy X-ray scattering data were collected at the Advanced Photon Source, Argonne National Laboratory (wiggler beamlines 11-ID-B and 11-ID-C BESSRC CAT). The concentration-dependent experiments were conducted on 11-ID-B running with an incident beam energy of 91 keV, which corresponds to a wavelength of 0.13702 Å. The scattered intensity was measured using a General Electric amorphous silicon flat-panel X-ray detector (GE Healthcare) mounted in a static position ($2\theta = 0°$) providing detection in momentum transfer space Q up to 32 $Å^{-1}$ at this fixed geometry. Redox speciation experiments were conducted on the wiggler beamline 11-ID-C[17] running with an incident beam energy of 115 keV, which corresponds to a wavelength of 0.108 Å. Samples were mounted in 3 mm glass capillaries that were further encapsulated with Kapton tape as required for actinide samples. The capillaries were mounted with their long axes perpendicular to both the incident beam and detector travel.[18] The experiment was performed in transmission geometry, which provides a constant path length as a function of scattering angle. Data were collected using a single-element Ge detector and covered the momentum transfer range of Q from about 0.3 to 30 $Å^{-1}$.

The data were corrected for detector dead time, background (with empty sample holder), polarization, and tangential detector movement. The data were normalized to a cross-section per formula unit and subtracted from background solutions containing LiOH in perchloric acid, following previously published procedures. Data were obtained on room temperature solutions and were treated as described previously.[19,20]

The X-ray data obtained in these experiments are equivalent to standard powder patterns, that is, intensity versus scattering angle, except that the data are taken out to large momentum transfers (Q). For example, a powder pattern obtained with a copper tube as the X-ray source has a maximum Q of about 8 $Å^{-1}$. This is important because the scattering data are Fourier-transformed to provide $g(r)$, a pair-correlation or pair distribution function (PDF), as a function of distance, r, the resolution of which is dependent on the Q range used in the Fourier transform (FT).[21,22] Peak positions in a PDF represent coordination distances between ions. The data shown in the figures are background-subtracted, which means that peaks in the $g(r)$ versus r plots represent coordination distances of neptunium to other atoms and their intensities are related to the relative concentrations of the correlated pairs.

Results and Discussion

Np−First Coordination Sphere. The background-subtracted scattering data from the neptunyl(V) and (VI) solutions are compared in Figure 2 as $S(Q)$ versus Q. Also shown in the figure are the PDFs, obtained by Fourier-transforming the $S(Q)$ data, with peaks that correspond only to the Np atomic correlations in solution. Except for the correlations observed in the $Np(V)O_2^+$ data at about 4.2 Å, the two PDFs are very similar, with the slight shift to shorter distances of the hexavalent neptunium data, relative to the pentavalent correlations, reflecting the smaller ionic radius of Np^{6+}. The metrical results are summarized in Table 1. There are three strong peaks in the PDF of the hexavalent sample. The first peak, at 1.74(2) Å, has an intensity corresponding to 16.4(5) electrons, determined from an

(15) Antonio, M. R.; Soderholm, L.; Song, I. *J. Appl. Electrochem.* **1997**, *27*, 784–792.
(16) Soderholm, L.; Antonio, M. R.; Williams, C.; Wasserman, S. R. *Anal. Chem.* **1999**, *71*, 4622–4628.
(17) Rutt, U.; Beno, M. A.; Strempfer, J.; Jennings, G.; Kurtz, C.; Montano, P. A. *Nucl. Instrum. Methods Phys. Res., Sect. A* **2001**, *467*, 1026–1029.
(18) Soderholm, L.; Skanthakumar, S.; Neuefeind, J. *Anal. Bioanal. Chem.* **2005**, *383*, 48–55.
(19) Skanthakumar, S.; Soderholm, L. *Mater. Res. Soc. Symp. Proc.* **2006**, *893*, 411–416.
(20) Skanthakumar, S.; Antonio, M. R.; Wilson, R. E.; Soderholm, L. *Inorg. Chem.* **2007**, *46*, 3485–3491.
(21) Magini, M.; Licheri, G.; Paschina, G.; Piccaluga, G.; Pinna, G. *X-ray diffraction of ions in aqueous solutions: hydration and complex formation*; CRC Press Inc.: Boca Raton, 1988.
(22) Egami, T.; Billinge, S. J. L. *Underneath the Bragg Peaks: Structural Analysis of Complex Materials*; Pergammon: Amsterdam, 2003.

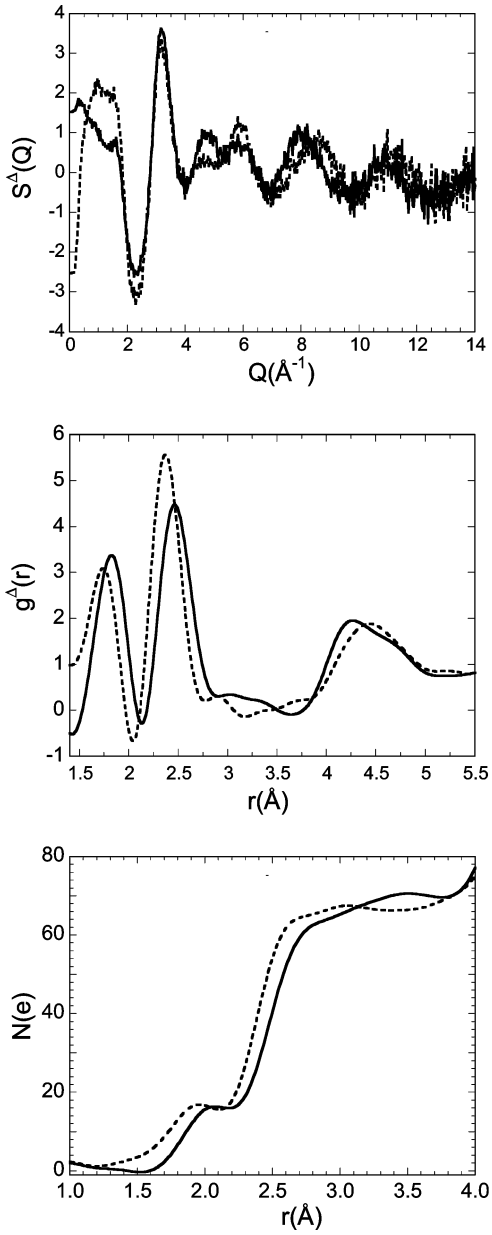

Figure 2. (Top) The background and solvent-corrected scattering from a single 0.4 M Np^{5+} (solid line) and Np^{6+} (dashed line) solution by electrochemical redox control. (Middle) The Fourier transform of the data shown above. The peak at about 1.7−1.82 Å corresponds to the dioxo ligands, 2.37−2.90 Å to the equatorial waters, and about 4.5 Å to the second coordination sphere of Np in solution. (Bottom) The integration of the real space scattering intensity as a function of distance, which produces peaks of 15.9(5) and 51(4) electrons for the first two peaks in the Np^{5+} spectrum and 16.4(5) and 49(2) electrons for the Np^{6+} spectrum. These values correspond to two O ligands and 5 waters, respectively.

Table 1. Fitted Parameters for the Pair Correlations Observed in the $g(r)$ vs r Patterns Shown in Figure 2

solution	r (Å)	integration (electrons)	coordination
NpO_2^+	1.82(2)	15.9(5)	2 oxo ligands
	2.46(2)	51(4)	5 H_2O
	4.2–4.6	varied (see text)	H_2O and Np
NpO_2^{2+}	1.74(2)	16.4(5)	2 oxo ligands
	2.37(2) 2.90(4)	49(2)	5 waters (5 O, 10 H)
	4.37(3)	80(20)	6−10 waters

integration of the peak shown in Figure 2. This correlation is assigned to the two Np−O correlations of the oxo ligands. The distance is consistent with previous reports on solution neptunyl(VI) speciation determined using EXAFS spectroscopy[23] and slightly shorter than the distance observed in the solid state.[24] The second peak, at 2.37(2) Å with a shoulder peak at 2.90(4) Å, is assigned to five equatorial water ligands (oxygen and hydrogen respectively) based on a total integration of 49(2) electrons. This result confirms earlier EXAFS results suggesting five waters in the equatorial coordination environment of NpO_2^{2+} under similar solution conditions.[23]

Analysis of the scattering data from $Np(V)O_2^+$ solutions gave similar results for the first coordination sphere. The first peak, attributed to the dioxo ligands, is found at 1.82(2) Å. It has an intensity that integrates to 15.9(5) electrons, which corresponds to two dioxo ligands (16 electrons) within the error of the measurement. Examination of the peak width shows that it is not significantly broadened compared to the corresponding peak from the Np(VI) sample. The second peak, at 2.46(2) Å, has a much broader high-r shoulder that indicates a disruption of the well-defined water orientation with respect to Np that is seen for neptunyl(VI). The neptunyl(V) shoulder appears to extend over the range of about 3−3.5 Å; its broadening is visible in the integration shown in Figure 2. The integration corresponds to 51(4) electrons, which represents an equatorial water coordination of 5. The Np−O distance is the same, within error, to that determined from an analysis of EXAFS data obtained from pentavalent Np solutions too dilute to have significant CCIs.[14,23,25–27] An EXAFS study on a more concentrated solution, 2.7 M Np, with observable CCIs[14] also has indistinguishable fit parameters. The occurrence of CCIs in the solid state results in Np−oxo bond distances over the range 1.77−1.89 Å, details of which are sensitive to the type of interaction.[28] The coordination number of five equatorial waters for NpO_2^+ is again consistent with the number found by the use of EXAFS spectroscopy.[23]

The HEXS results on the first coordination sphere environment for $Np(VI)O_2^{2+}$ and $Np(V)O_2^+$ in solution are consistent with known uranyl and neptunyl solid-state structural information.[1,28]

Neptunyl−Second Coordination Sphere. There are additional correlations observable in the FT over the distance range 3.5−4.5 Å. Interactions have been observed previously in HEXS data from Th,[29,30] uranyl,[18,31,32] and Cm,[20] where they have been attributed to correlations between the dissolved metal ion and waters in its second-coordination sphere. Following these precedents, the peak from the neptunyl(VI) FT centered at about 4.4 Å is assigned to second-coordination sphere Np−H_2O interactions. Complicating the quantitative analysis of this peak is the onset of

(23) Antonio, M. R.; Soderholm, L.; Williams, C. W.; Blaudeau, J. P.; Bursten, B. E. *Radiochim. Acta* **2001**, *89*, 17–25.
(24) Forbes, T. Z.; Burns, P. C. *Can. Mineral.* **2007**, *45*, 471–477.
(25) Combes, J. M.; Chisholm-Brause, C. J.; Brown, G. E., Jr.; Parks, G. A.; Conradson, S. D.; Eller, P. G.; Triay, I. R.; Hobart, D. E.; Miejer, A. *Environ. Sci. Technol.* **1992**, *26*, 376–382.
(26) Allen, P. G.; Bucher, J. J.; Shuh, D. K.; Edelstein, N. M.; Reich, T. *Inorg. Chem.* **1997**, *36*, 4676–4683.
(27) Reich, T.; Bernhard, G.; Geipel, G.; Funke, H.; Hennig, C.; Rossberg, A.; Matz, W.; Schell, N.; Nitsche, H. *Radiochim. Acta* **2000**, *88*, 633–637.
(28) Krot, N. N.; Grigoriev, M. S. *Russ. Chem. Rev.* **2004**, *73*, 89–100.

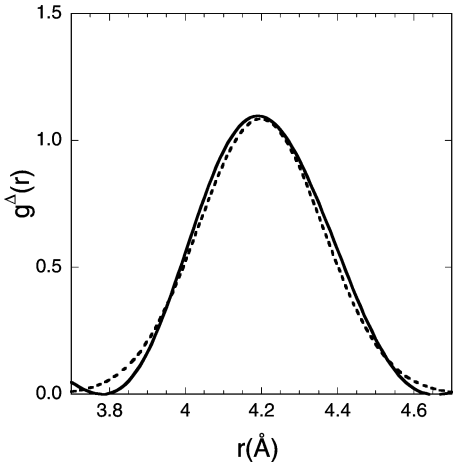

Figure 3. The scattering contribution from the neptunyl(V) CCI after subtracting the contributions from the water scattering (solid line) compared to a Gaussian centered at 4.20(5) Å and with a height of 1.09.

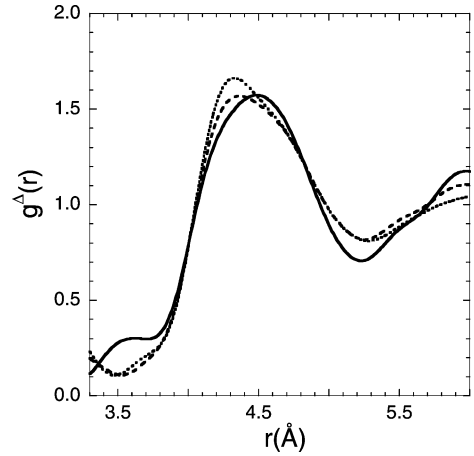

Figure 4. The variation of scattering intensity with Np^{5+} concentration for 0.059 (solid line), 0.118 (dashed line), and 0.236 M (dotted line) solutions.

solvent−solvent and solvent−other-ligand correlations that develop over the same distance range and must be subtracted from the data. This is accomplished by subtracting either a linear background or a background represented by an arctangent function over the distance range 3.2−5.6 Å. The arctan-subtracted peak is well-represented as a Gaussian centered at 4.37(3) Å, the integration of which results in the determination of 6−10 water molecules correlated to Np over this distance range. This result can be compared to the 10 waters found associated with the dissolved uranyl ion in its second coordination sphere, where it was suggested that there could be five waters correlating above the equatorial plane of the dioxo moiety and five waters below the plane.[18]

The corresponding region in the neptunyl(V) spectrum is more complex; there is an unresolved peak to the low-*r* side of the intensity centered at about 4.45(10) Å that is attributed to Np−Np correlations associated with CCIs. Quantification of this scattering was done by simply subtracting the water correlations determined from the neptunyl(VI) data. The scattering contribution obtained following this procedure, together with its Gaussian fit, is shown in Figure 3. The peak attributable to Np CCIs is centered at 4.20(5) Å, the same distance seen in wide-angle X-ray scattering (WAXS) data, where it was assigned to pentavalent Np−Np interactions in a perchloric acid solution with an ionic strength of 0.5 M.[12] It was pointed out in the discussion of the WAXS results that the Np−Np distance alone was not sufficient to distinguish between two different interaction models, designated Model I and Model II, as depicted in Figure 1. EXAFS data obtained from similar solutions showed evidence of a weak Np−Np interaction.[14] Including the appropriate multiple scattering paths for the two models resulted in a distance of 4.20(3) Å for CCI Model I and 4.00(3) Å for the dihydroxo bridging seen in Model II. The HEXS data confirm the interaction distance of 4.20 Å and can be used to support the Model I results from the EXAFS fitting. There are numerous solid-state structural studies of Np compounds that exhibit CCIs.[28,33–38] The Np−Np bond distances have a broad range, 3.95−4.3 Å, which reflects the different geometry of the interaction. In contrast, the dihydroxo bridged Np−$(OH)_2$−Np interaction is about 3.98 Å.[37] Taken together, the results strongly support the Np−Np interaction via CCIs, as depicted in Model I, Figure 1a.

Np(V)−Np(V) Stability Constant. The intensity of the peak at 4.20(5) Å in Figure 3, which is attributed to a Np−Np CCI dimer correlation, can be used to estimate the relative number of Np−Np dimers in solution. Assuming a simple equilibrium between the monomer and dimer, the stability constant K_{eq} of the dimer interaction can then be estimated from

$$K_{eq} = \frac{[\text{dimer}]}{[\text{monomer}]^2} \quad (1)$$

This was done by first using the Np(VI) pattern to remove contributions from the second coordination water over the range 3.2−5.6 Å, thus isolating the Np−Np scattering. Integrating reveals 24−30 electrons involved in the remaining scattering, which corresponds to an average Np coordination number between 0.26 and 0.32 Np. From this average number, a stability constant for the monomer−dimer equilibrium of 0.74(9) M^{-1} is obtained. This value was tested by determining the average Np CCIs as a function of concentration. Additional HEXS data obtained from solutions containing 0.059, 0.118, and 0.236 M Np are shown in Figure 4. An average Np−Np coordination of 0.07 is calculated for

(29) Wilson, R. E.; Skanthakumar, S.; Burns, P. C.; Soderholm, L. *Angew. Chem., Int. Ed.* **2007**, *46*, 8043–8045.
(30) Wilson, R. E.; Skanthakumar, S.; Sigmon, G.; Burns, P. C.; Soderholm, L. *Inorg. Chem.* **2007**, *46*, 2368–2372.
(31) Neuefeind, J.; Soderholm, L.; Skanthakumar, S. *J. Phys. Chem. A* **2004**, *108*, 2733–2739.
(32) Aberg, M.; Ferri, D.; Glaser, J.; Grenthe, I. *Inorg. Chem.* **1983**, *22*, 3986–3989.
(33) Albrecht-Schmitt, T. E.; Almond, P. M.; Sykora, R. E. *Inorg. Chem.* **2003**, *42*, 3788–3795.
(34) Forbes, T. Z.; Burns, P. C. *J. Solid State Chem.* **2005**, *178*, 3445–3452.
(35) Andreev, G. B.; Antipin, M. Y.; Budantseva, N. A.; Krot, N. N. *Russ. J. Coord. Chem.* **2005**, *31*, 800–803.
(36) Grigor'ev, M. S.; Antipin, M. Y.; Krot, N. N. *Radiochemistry (New York)* **2006**, *48*, 6–10.
(37) Almond, P. M.; Skanthakumar, S.; Soderholm, L.; Burns, P. C. *Chem. Mater.* **2007**, *19*, 280–285.
(38) Forbes, T. Z.; Burns, P. C.; Skanthakumar, S.; Soderholm, L. *J. Am. Chem. Soc.* **2007**, *129*, 2760–2761.

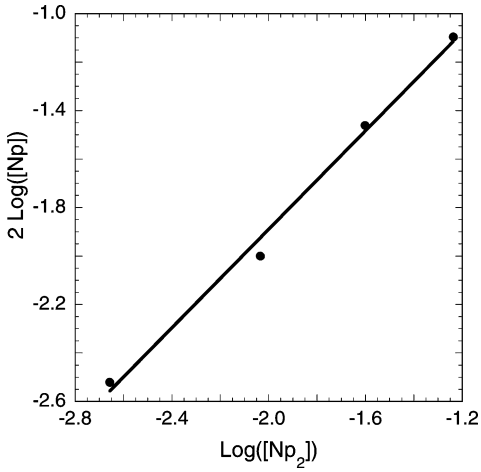

Figure 5. The concentrations of the Np monomer plotted vs the Np CCI dimer. The line, representing the best fit to the data, has a slope of 1, indicating a well-behaved solution. The intercept is used to determine the stability constant of 0.74(9) M^{-1} for the CCI complex.

the 0.059 M solution from the stability constant of 0.74 M^{-1} and can be seen as a slight asymmetry to the scattering peak. Average coordinations for the remaining samples are determined by using this solution as a background. This method may slightly underestimate the dimer concentration if the coordination number in the second coordination sphere decreases with dimerization, an uncertainty that has been included in our reported error. A plot of the resulting monomer-to-dimer ratios as shown in Figure 5 can be used to assess the stability constant determined from the initial 0.4 M solution. The plot corresponds to $\log(K_{eq}) = \log([\text{dimer}]) - 2\log([\text{monomer}])$ such that the slope as plotted is 1.01(1), consistent with the slope of 1 expected for a well-behaved system. The intercept of the best fit line is 0.74(9) and corresponds to the stability constant for the CCI dimer. This value is the same, within error, as the estimate from the 0.4 M Np solution. The excellent fit to the data, combined with the resulting ideal slope, confirms that the solution is well-behaved over the concentrations used in this experiment and that there is no evidence of higher oligomer formation. As shown by the comparisons listed in Table 2, this result is also consistent with the stability constant of Np−Np CCIs determined using Raman and optical absorption spectroscopy,[11,13] as well as density functional theory.[9]

Table 2. Stability Constants Obtained for the Np−Np Dimer Depicted in Figure 1a

ionic strength (M)	stability constant K_{eq}	technique	ref
1	0.74(9)	HEXS	this work
4.26	0.82(5)	Raman absorption	11
6.0	1.41(14)	absorption	13
	0.73	DFT calculation	9

Conclusions

The analysis of HEXS data from acidic $Np(V)O_2^+$ and $Np(VI)O_2^{2+}$ perchlorate solutions confirms that the central metal is coordinated with five equatorial waters in both cases. The data also show a second coordination sphere that, for neptunyl(VI), is comprised of 6−10 water molecules at a distance of about 4.37 Å. The neptunyl(V) second coordination sphere is more complex; in addition to coordinating waters, there is also a peak at about 4.20 Å that changes intensity with changing Np concentration. This peak is not visible in the Np(VI) data and is attributed to evidence of cation−cation interactions. Comparisons of the Np−Np distance with known solid-state structures supports the T-shaped configuration for this interaction, in which the oxo moiety of one neptunyl(V) is coordinated in the equatorial plane of a neighboring neptunyl. A quantitative analysis of the scattering intensity from the Np−Np CCI as a function of neptunium concentration finds a stability constant, $K_{eq} = 0.74(9)\ M^{-1}$, in general agreement with previous literature reports.

Acknowledgment. This work was funded by the U.S. Department of Energy, OBES, Chemical Sciences, under Contract DE-AC02-06CH11357 to Argonne National Laboratory. The HEXS data were measured at beamline 11-ID-B of the Basic Energy Sciences Synchrotron Radiation Center (BESSRC), Advanced Photon Source (APS). Use of the Advanced Photon Source is supported by the U.S. Department of Energy, Office of Science, OBES, Materials Sciences, also under Contract No. DE-AC02-06CH11357.

IC702478W